Electronic Supplementary Material (ESI) for New Journal of Chemistry.

Electronic Supplementary Information

CARBAZOLE/FLUORENE SUBSTITUTED 5-PHENYL-2,2'-BIPYRIDINE D-π-A FLUOROPHORES: PHOTOPHYSICAL DATA, HYPERPOLARIZABILITY AND CT-INDICES

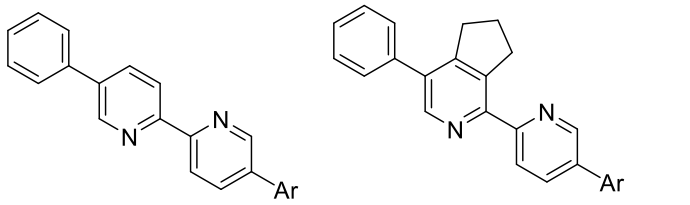

Ar = H
Ar = 3-OMe-C_6H_4,
Ar = 4-OMe-C_6H_4
Ar = 3,4,5-tri(MeO)C_6H_2

Ar = 3-OMe-C_6H_4,
Ar = 4-(Ph_2N)C_6H_4
Ar = 3,4,5-tri(MeO)C_6H_2
Ar = Ph

Figure S1 The structures of 5,5′-diaryl-2,2′-bipyridines fluorophores reported previously by our group[1,2]

Materials, equipments, measurements and characterization methods

UV-vis absorption spectra were recorded on the Shimadzu UV-1800 spectrophotometer using quartz cells with 1 cm path length at room temperature. Emission and excitation spectra were measured on a Horiba FluoroMax-4 using quartz cells with 1 cm path length at room temperature. Absolute quantum yields for compounds **6a-c** and **7a-c** were obtained by the Integrating Sphere Quanta-φ of the Horiba-Fluoromax-4. Time-resolved fluorescence measurements were carried out using time-correlated single-photon counting (TCSPC) with a nanosecond LED (370 nm). ^{1}H NMR and ^{13}C NMR spectra were recorded on the Bruker Avance-400 spectrometer at 298 K, digital resolution ±0.01 ppm. Chemical shifts are expressed in parts per million (δ) and are referenced to tetramethylsilane (TMS) as internal standard and the signals were reported as s (singlet), d (doublet), t (triplet), m (multiplet), and coupling constants J were given in Hz. Mass-spectra were recorded on GCMS-QP2010 Ultra (Shimadzu). TLC was done on silica gel coated aluminum slide (Merck, Silica gel G for TLC). Silica gel (60–120 mesh, SRL, India) was used for column chromatography. All solvents were dried and distilled before use. Commercially available substrates were freshly distilled before the reaction. Solvents, reagents, and chemicals were purchased from Aldrich, Fluka, Merck, SRL, Spectrochem, and Process Chemicals. All reactions involving moisture-sensitive reactants were executed using oven-dried glassware.

Photoluminescence absolute quantum yield (PLQY) measurement

For each sensor was measured of absorption spectrum so that the concentration of solution was less 0,1 of optical density at selected wavelength to minimize inner-filter effect. For blank (naked solvent) and sensor solution were recorded of emission and Rayleigh scattering spectra by using Integrating Sphere of HORIBA FluoroMax-4. PLQY was calculated by equation:

$$\varphi = (E_c - E_a)/(L_a - L_c),$$

where E_c and L_c are the integrated luminescence of the sensor and blank, E_a and L_a are the integrated excitation profile of the sensor and blank.

Time-correlated single-photon counting (TCSPC)

For sensors was measured of absorption spectrum so that the concentration of solution was less 0,1 of absorption intensity at selected wavelength. Time-resolved fluorescence measurements were carried out using time-correlated single-photon counting (TCSPC) with a nanosecond LED (310 nm).

Table S1. Fluorescence lifetime of probes **6a-c** and **7a-c** (C = 2×10^{-6} M) in MeCN at r.t.

Entry	Compound	τ_1, ns[a]	α_1[b]	τ_2, ns[a]	α_2[b]	τ_{av}, ns[a]	χ^2[d]
1	**7a**	1.55	0.1952	3.35	0.8048	3.4	0.95
2	**7b**	1.26	0.2739	2.61	0.7261	2.6	0.90

3	**7c**	0.82	0.7984	1.64	0.2016	1.6	0.83
4	**6a**	1.25	0.2829	2.77	0.7171	2.8	0.87
5	**6b**	1.17	0.3226	2.46	0.6774	2.5	0.92
6	**6c**	0.75	0.8508	1.53	0.1492	1.5	1.17

[a] Decay time, [b] Fractional contribution, [c] Weighted average decay time $\tau_{av} = \Sigma (\tau_i \times \alpha_i)$, [d] Quality of fitting

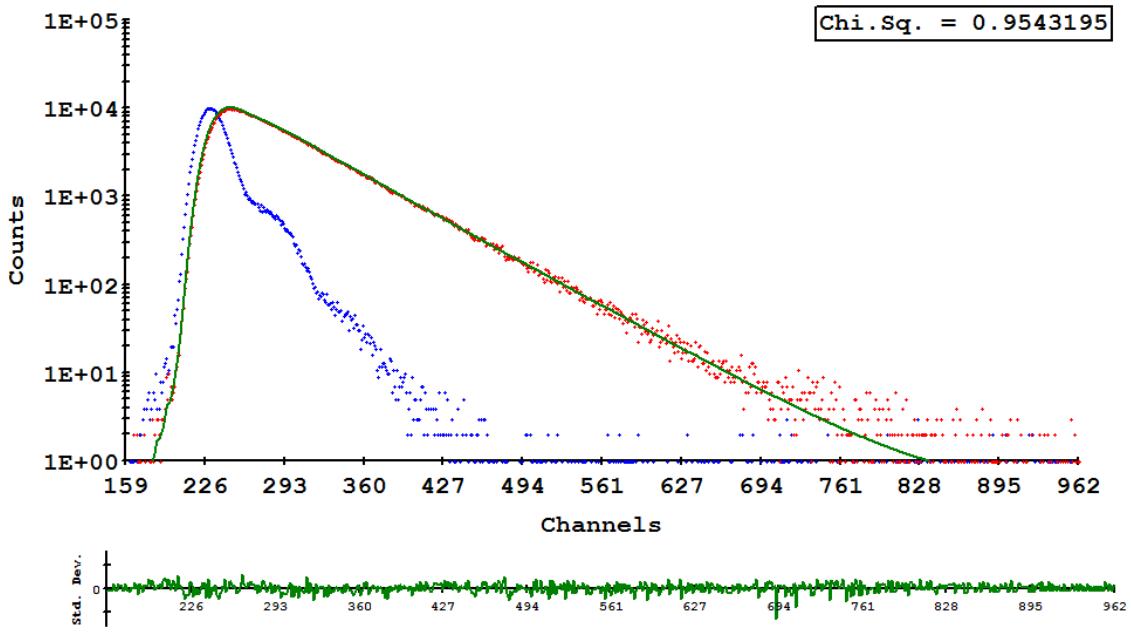

Figure S2 TCSPC measurement of compound **7a** in MeCN with corresponding residuals and χ^2

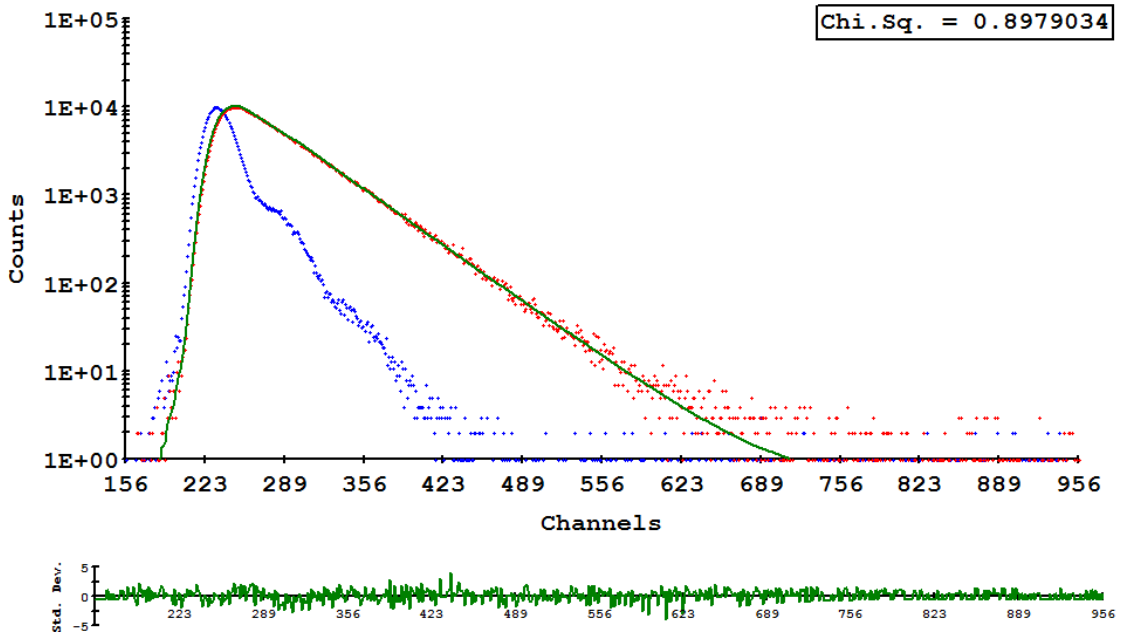

Figure S3 TCSPC measurement of compound **7b** in MeCN with corresponding residuals and χ^2

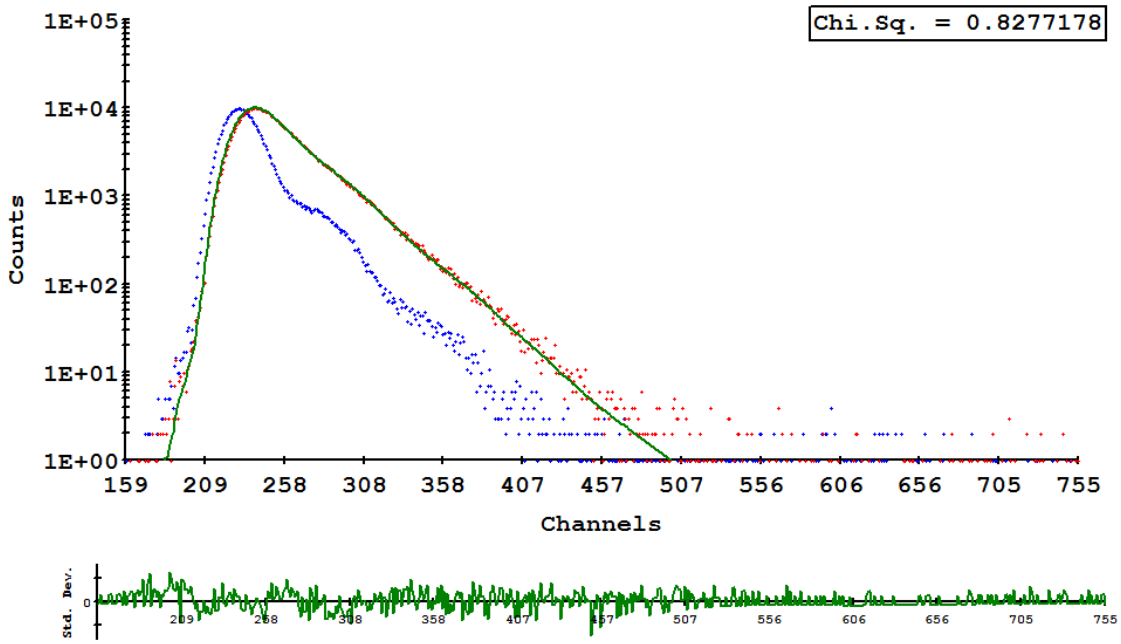

Figure S4 TCSPC measurement of compound **7c** in MeCN with corresponding residuals and χ^2

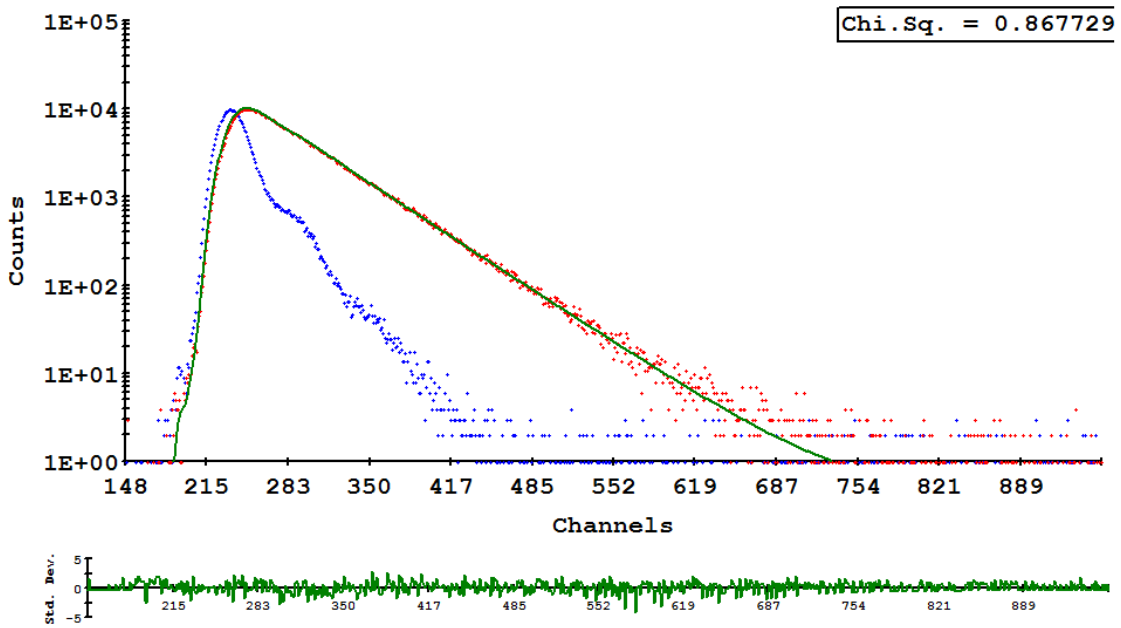

Figure S5 TCSPC measurement of compound **6a** in MeCN with corresponding residuals and χ^2

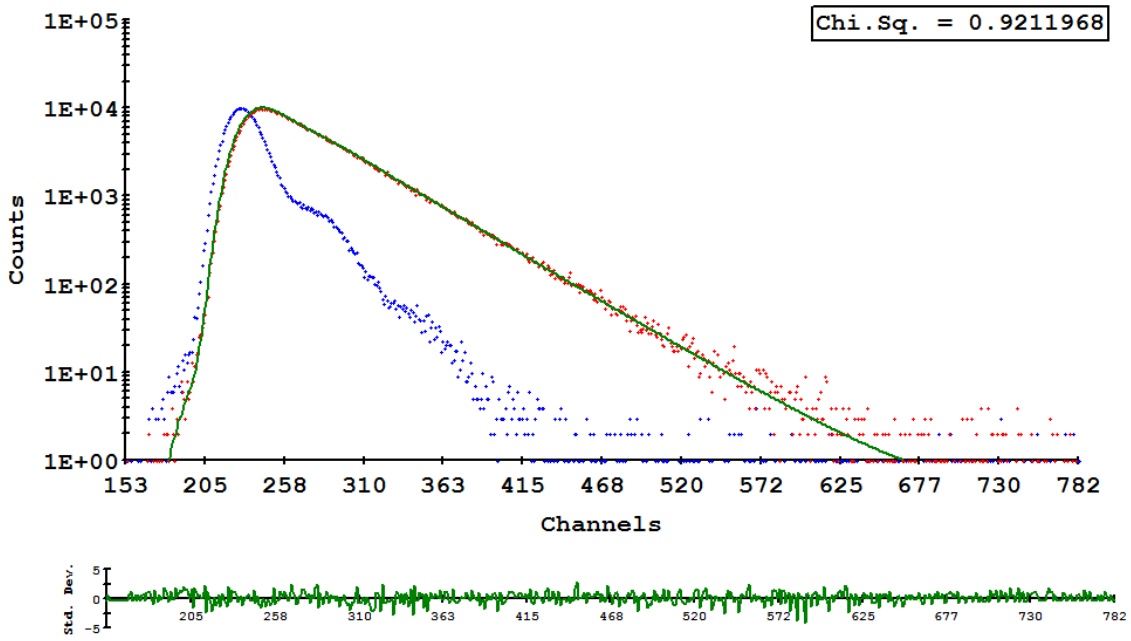

Figure S6 TCSPC measurement of compound **6b** in MeCN with corresponding residuals and χ^2

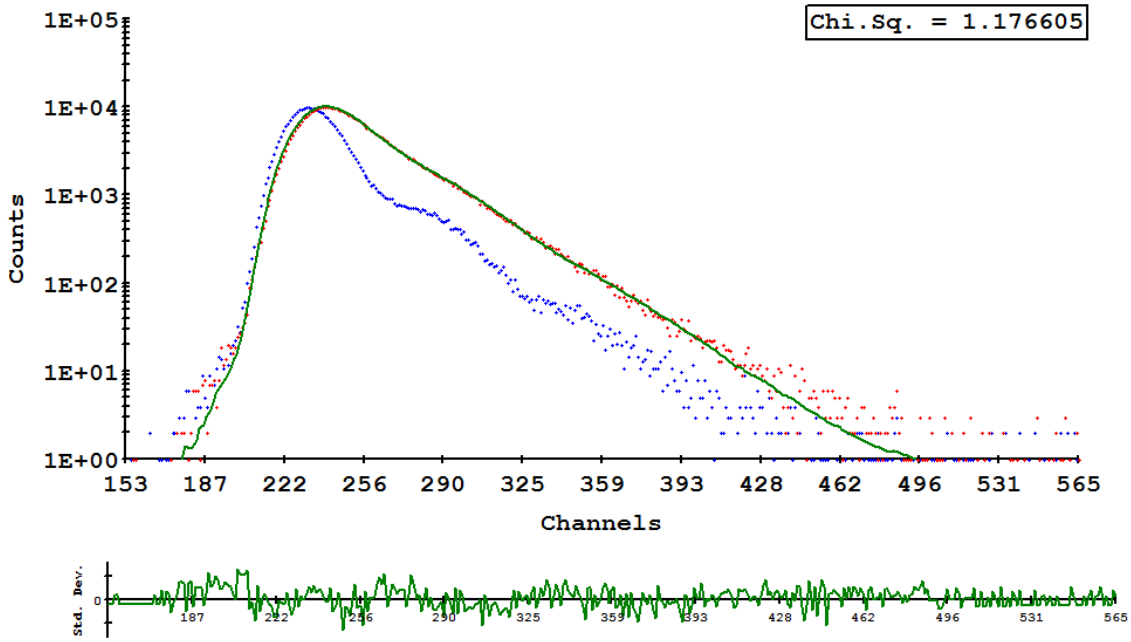

Figure S7 TCSPC measurement of compound **6c** in MeCN with corresponding residuals and χ^2

Table S2. Orientation polarizability for solvents (Δf), UV/Vis absorption and fluorescence emission maxima and Stokes shift of **6a** in different solvents

Solvent	Δf	λ_{abs}, nm	λ_{em}, nm	Stokes shift, cm^{-1} (nm)
Cyclohexane	0.001	321	369	4052 (48)
Toluene	0.013	322	379	4671 (57)
1,4-Dioxane	0,131	316	388	5872 (72)
CH_2Cl_2	0.218	318	409	6997 (91)
DMSO	0.26	320	454	9223 (134)
DMF	0.27	324	440	8137 (116)
MeCN	0.304	314	442	9324 (128)

Table S3 Orientation polarizability for solvents (Δf), UV/Vis absorption and fluorescence emission maxima and Stokes shift of **6b** in different solvents

Solvent	Δf	λ_{abs}, nm	λ_{em}, nm	Stokes shift, cm^{-1} (nm)
Cyclohexane	0.001	320	370	4223 (50)
Toluene	0.013	324	393	5419 (69)
1,4-Dioxane	0,131	322	398	5930(76)
CH_2Cl_2	0.218	321	425	7623 (10)
DMSO	0.26	328	484	9827 (156)
DMF	0.27	327	478	9660 (151)
MeCN	0.304	322	475	10394 (153)

Table S4 Orientation polarizability for solvents (Δf), UV/Vis absorption and fluorescence emission maxima and Stokes shift of **6c** in different solvents

Solvent	Δf	λ_{abs}, nm	λ_{em}, nm	Stokes shift, cm^{-1} (nm)
Cyclohexane	0.001	320	366	3928 (46)
Toluene	0.013	327	372	3699 (45)
1,4-Dioxane	0,131	324	377	4339 (53)
CH_2Cl_2	0.218	323	391	5384 (68)
DMSO	0.26	326	406	6044 (80)
DMF	0.27	327	398	5455 (71)
MeCN	0.304	320	398	6124 (78)

Table S5 Orientation polarizability for solvents (Δf), UV/Vis absorption and fluorescence emission maxima and Stokes shift of **7a** in different solvents

Solvent	Δf	λ_{abs}, nm	λ_{em}, nm	Stokes shift, cm^{-1} (nm)
Cyclohexane	0.001	326	375	4008 (49)
Toluene	0.013	330	390	4662 (60)
1,4-Dioxane	0,131	328	397	5299 (69)
CH_2Cl_2	0.218	326	424	7090 (98)
DMSO	0.26	330	481	9513 (151)
DMF	0.27	330	471	9071 (141)

MeCN	0.304	323	476	10048 (154)

Table S6 Orientation polarizability for solvents (Δf), UV/Vis absorption and fluorescence emission maxima and Stokes shift of **7b** in different solvents

Solvent	Δf	λ_{abs}, nm	λ_{em}, nm	Stokes shift, cm^{-1} (nm)
Cyclohexane	0.001	326	381	4428 (55)
Toluene	0.013	335	399	4788 (64)
1,4-Dioxane	0,131	333	410	5640 (77)
CH_2Cl_2	0.218	333	468	8662 (135)
DMSO	0.26	339	504	9657 (165)
DMF	0.27	333	495	9828 (162)
MeCN	0.304	331	496	10050 (165)

Table S7 Orientation polarizability for solvents (Δf), UV/Vis absorption and fluorescence emission maxima and Stokes shift of **7c** in different solvents

Solvent	Δf	λ_{abs}, nm	λ_{em}, nm	Stokes shift, cm^{-1} (nm)
Cyclohexane	0.001	326	369	3575 (43)
Toluene	0.013	329	378	3940 (49)
1,4-Dioxane	0,131	328	381	4241 (53)
CH_2Cl_2	0.218	329	398	5269 (69)
DMSO	0.26	334	418	6017 (84)
DMF	0.27	332	404	5368 (72)
MeCN	0.304	327	407	6011 (80)

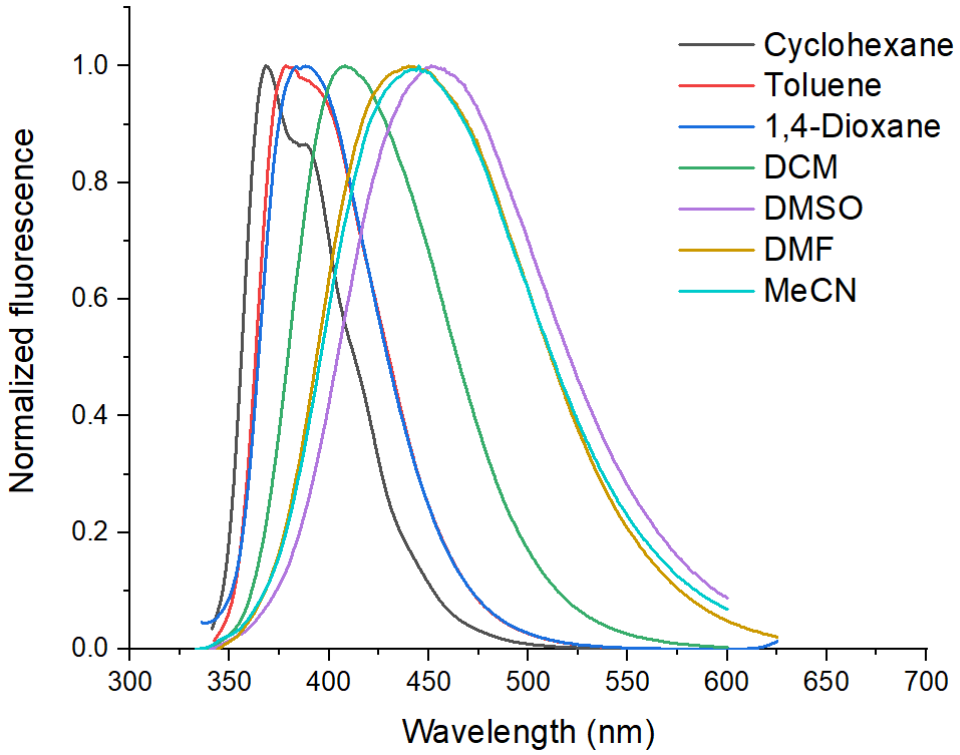

Figure S8 Normalized fluorescence emission spectra of **6a** in solvents with different polarity (c= 10^{-5} M^{-1})

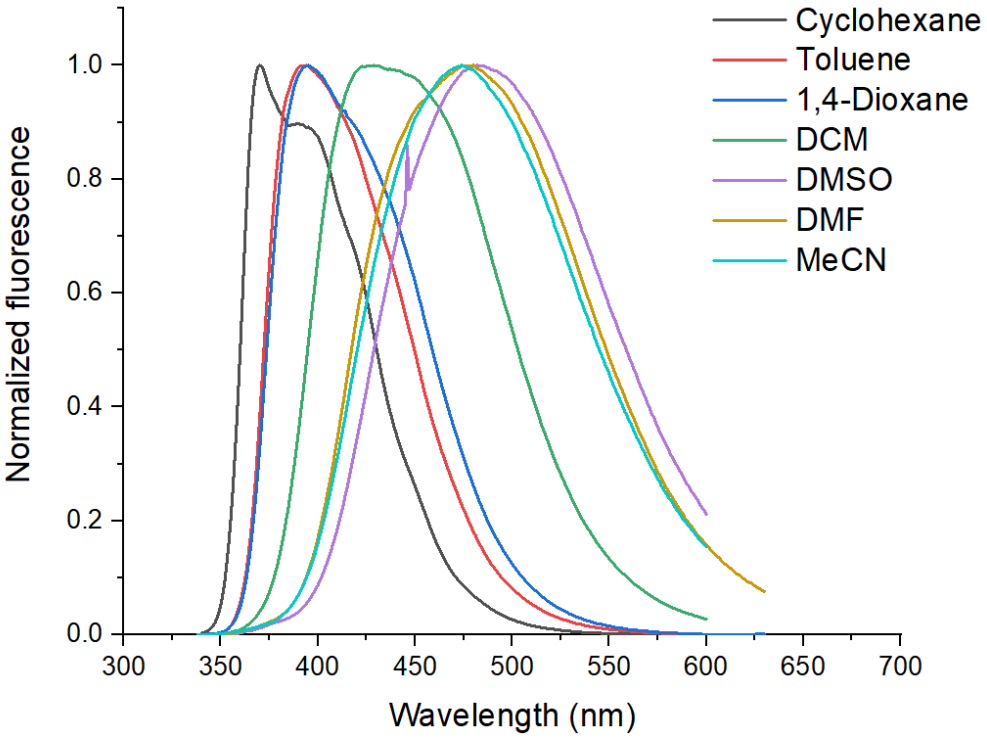

Figure S9 Normalized fluorescence emission spectra of **6b** in solvents with different polarity (c= 10^{-5} M^{-1})

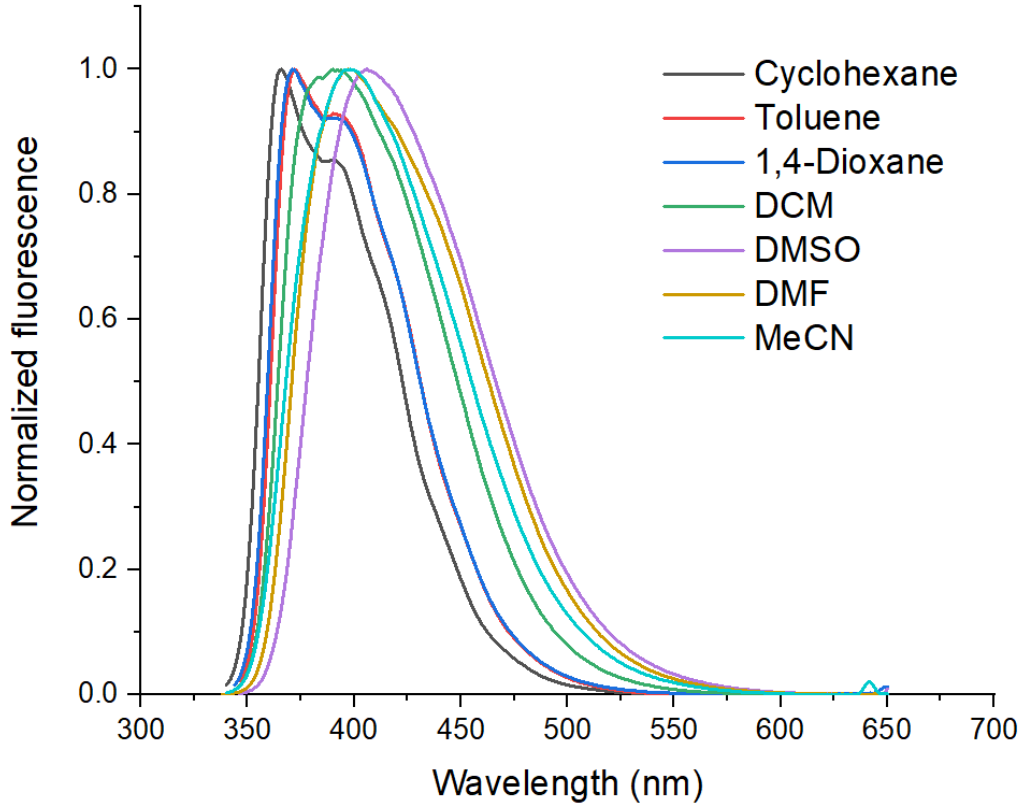

Figure S10 Normalized fluorescence emission spectra of **6c** in solvents with different polarity (c= 10^{-5} M^{-1})

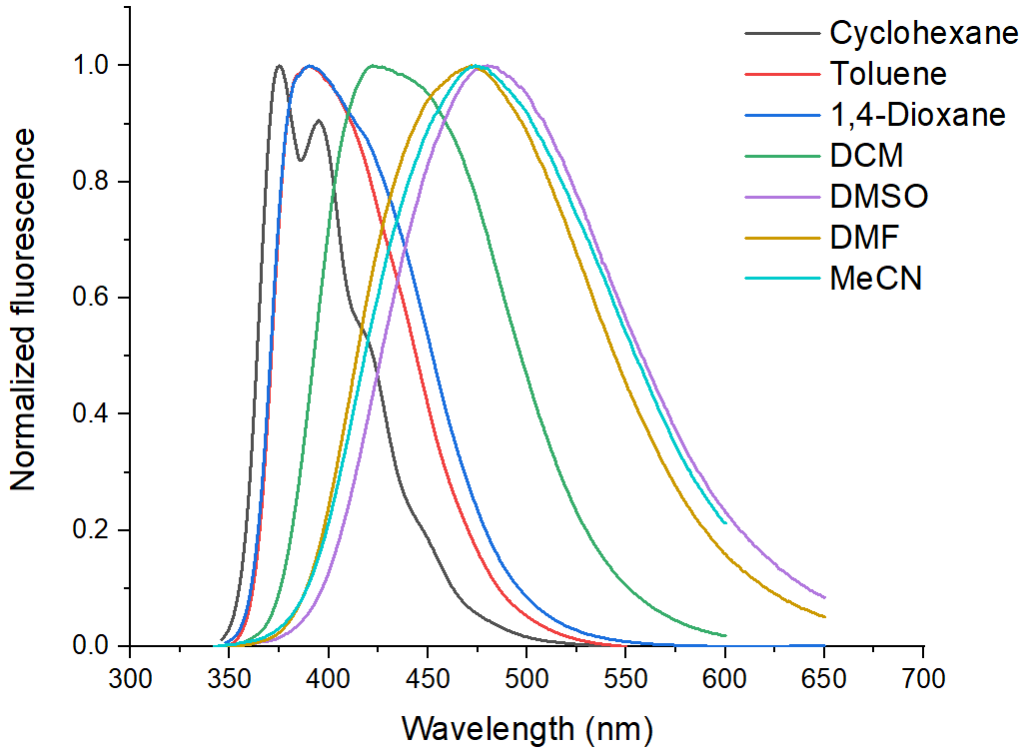

Figure S11 Normalized fluorescence emission spectra of **7a** in solvents with different polarity (c= 10^{-5} M^{-1})

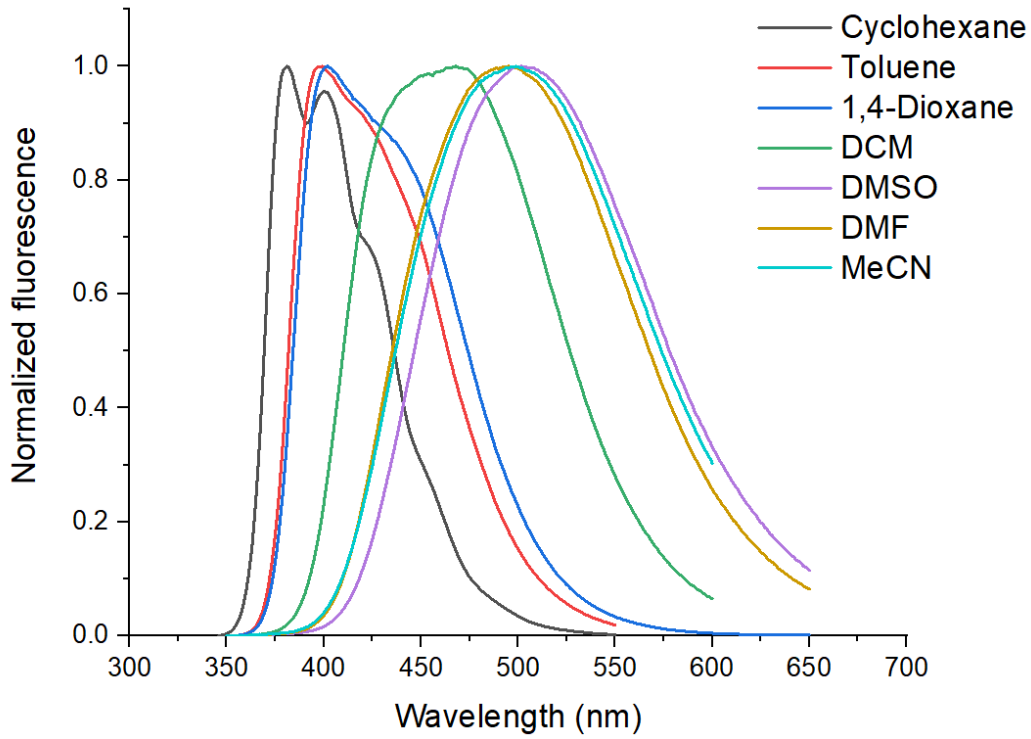

Figure S12 Normalized fluorescence emission spectra of **7b** in solvents with different polarity (c= 10^{-5} M^{-1})

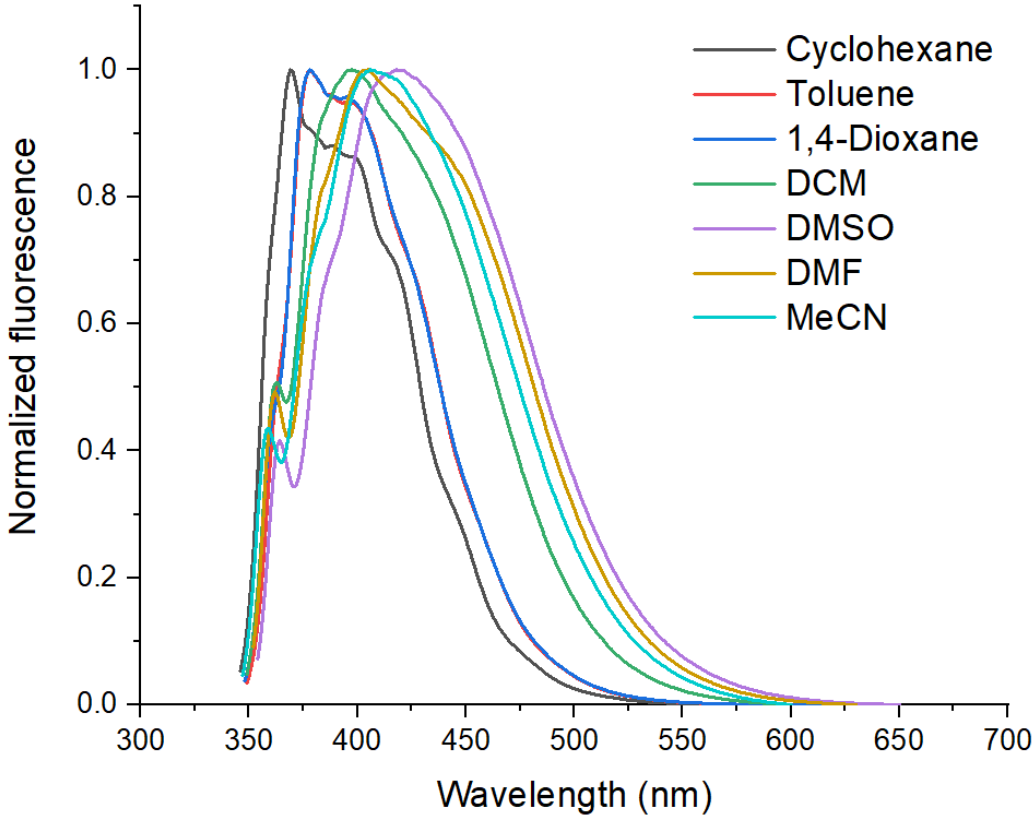

Figure S13 Normalized fluorescence emission spectra of **7c** in solvents with different polarity (c= 10^{-5} M^{-1})

$$D_X = |X_{ele} - X_{hole}| \quad \text{(S1)}$$

$$D_Y = |Y_{ele} - Y_{hole}| \quad \text{(S2)}$$

$$D_Z = |Z_{ele} - Z_{hole}| \quad \text{(S3)}$$

$$D\ index = \sqrt{(D_X)^2 + (D_Y)^2 + (D_Z)^2} \quad \text{(S4)}$$

$$H_\lambda = \frac{(\sigma_{ele,\lambda} + \sigma_{hole,\lambda})}{2\lambda} = \{x, y, z\} \quad \text{(S5)}$$

$$H_{CT} = |H\mu_{CT}| \quad \text{(S6)}$$

$$H\ index = \frac{(|\sigma_{ele}| + |\sigma_{hole}|)}{2} \quad \text{(S7)}$$

$$t\ index = D_{index} - H_{CT} \quad \text{(S8)}$$

$$\Lambda\ index = \int \Lambda(r)dr \equiv \int \sqrt{p^{hole}(r)\, p^{ele}(r)\, dr} \quad \text{(S9)}$$

Equations S1-S9. CT-indices calculations, where X, Y, Z (Equations S1-S3) refer to the centroid coordinates of holes and electrons, respectively.

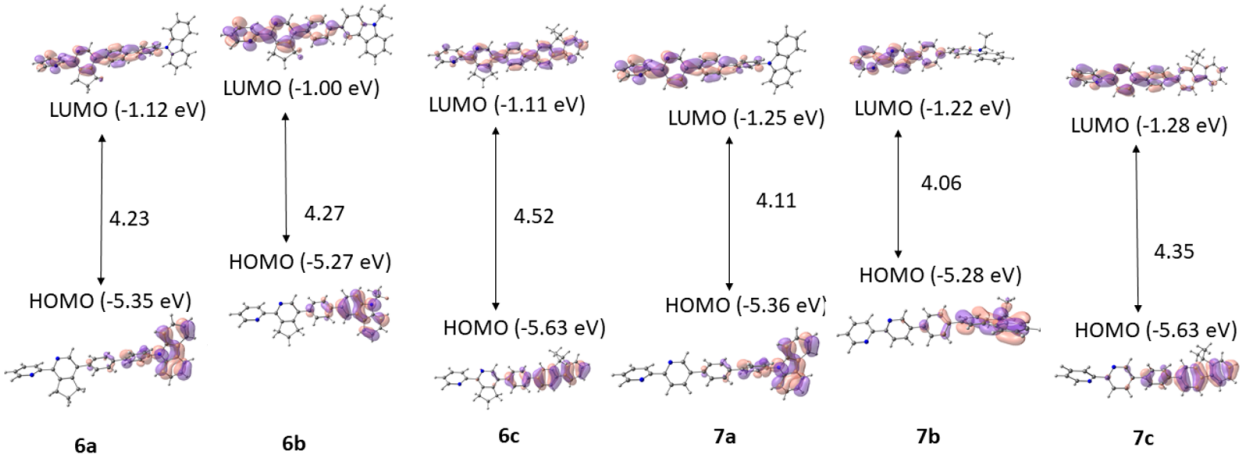

Figure S14. Frontier molecular orbitals and the energy level diagrams for **6a-c** and **7a-c** in MeCN.

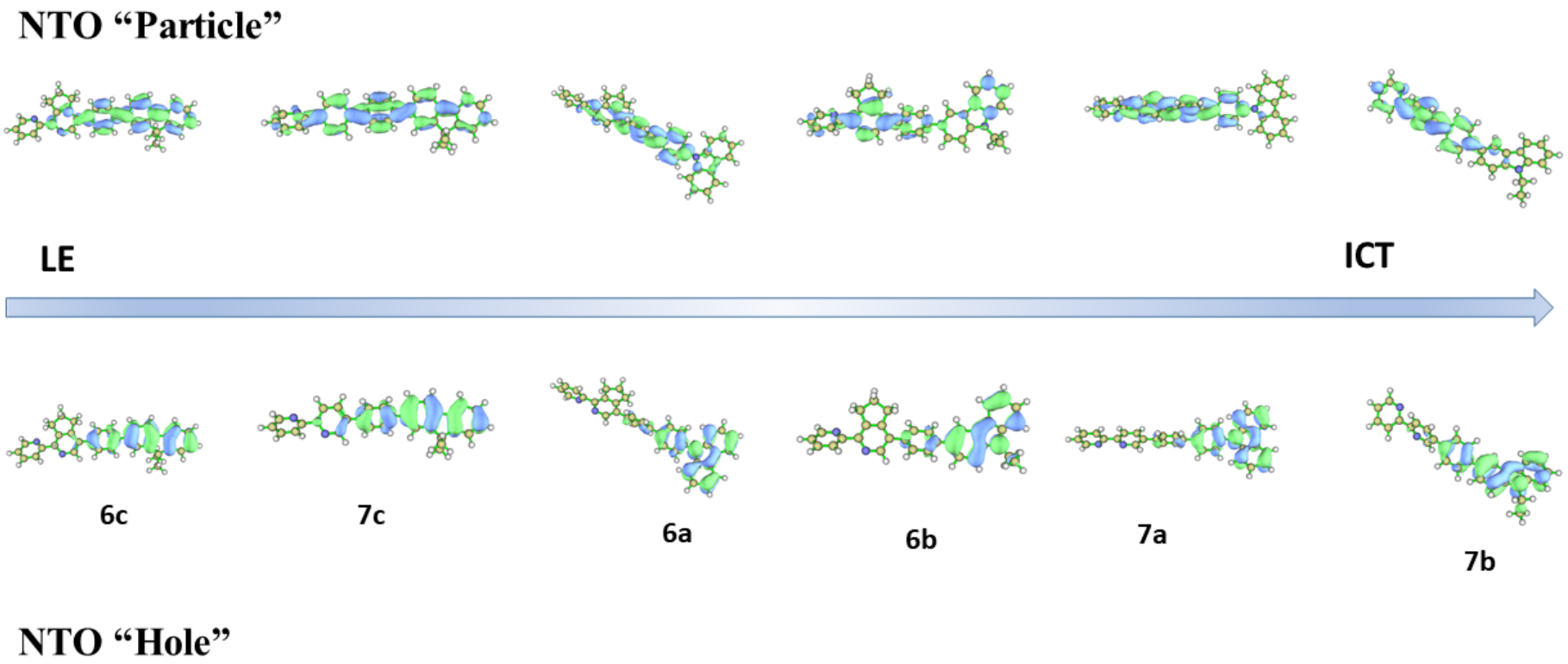

Figure S15. Calculated natural transition orbitals for **6a-c** and **7a-c**

Table S8. HOMO/LUMO electron density distribution and optimized structures in S_0 in MeCN and visualization of the MEP Distribution

	HOMO/LUMO electron density distribution	Optimized Structures in S_0 in MeCN and visualization of the Molecular Electrostatic Potential Distribution
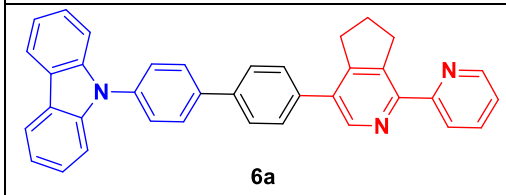 6a	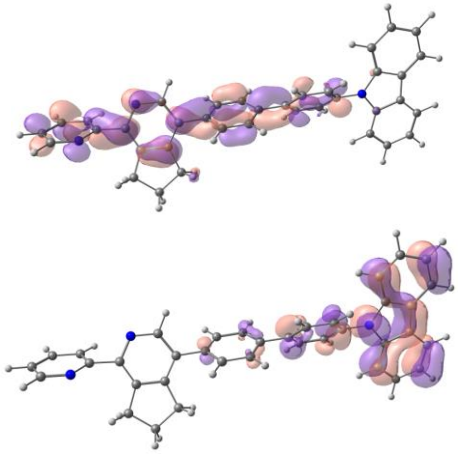	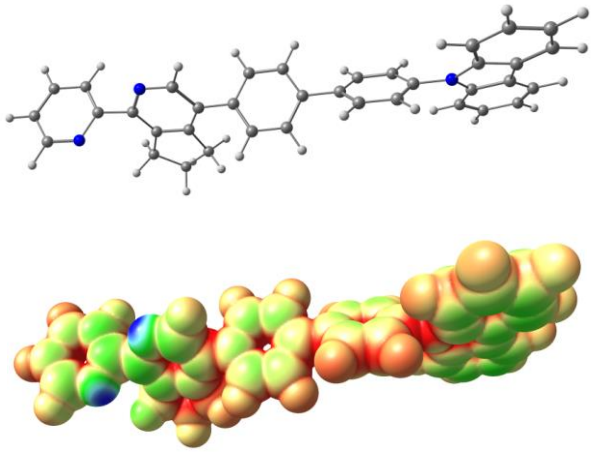
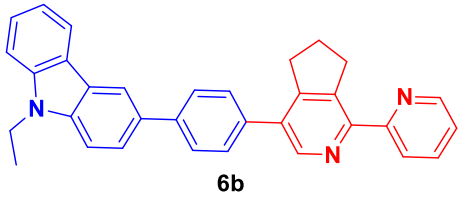 6b	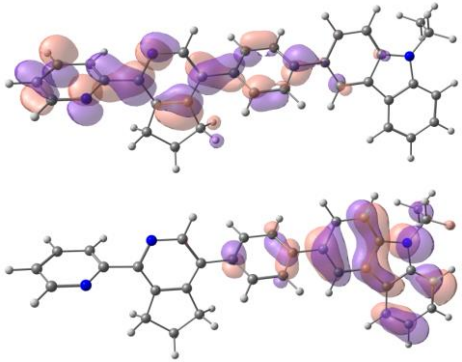	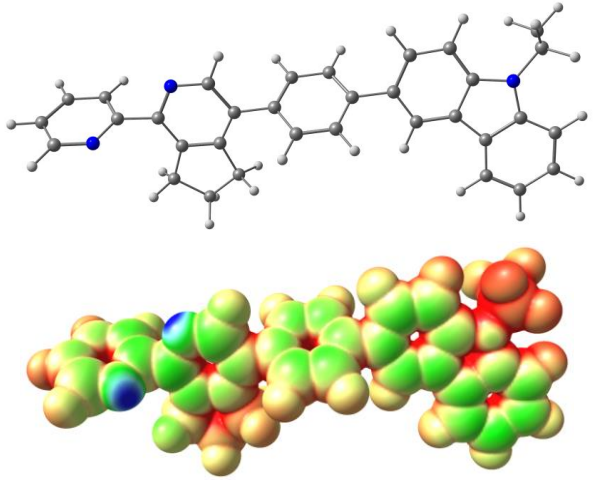

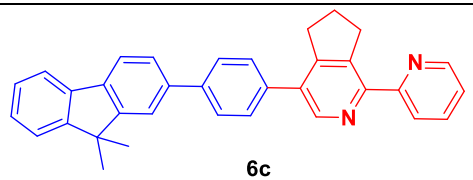 6c	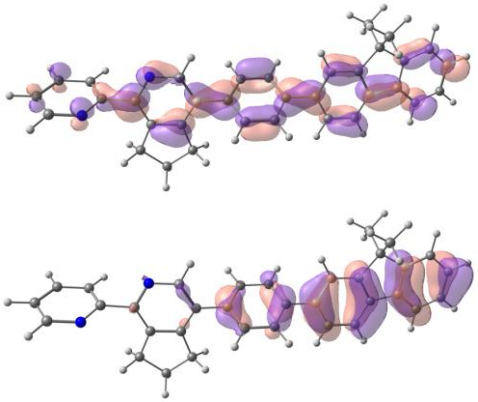	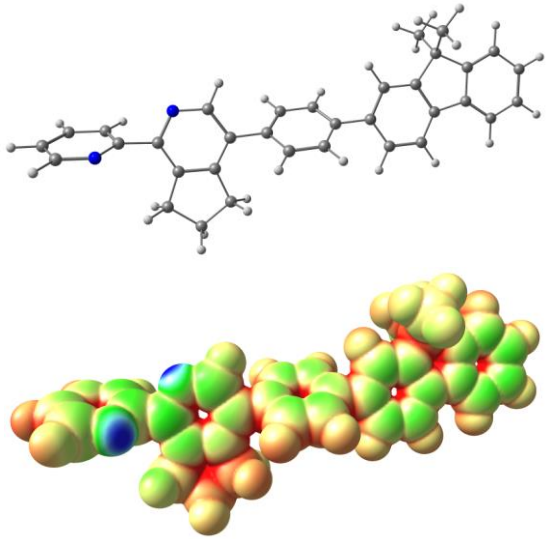
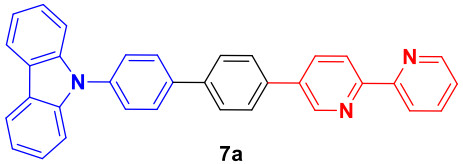 7a	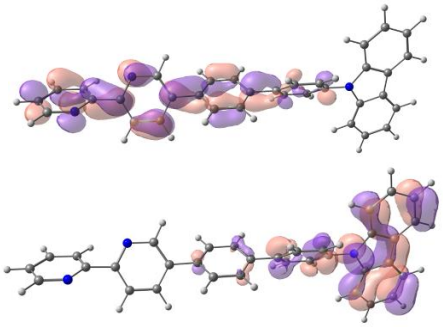	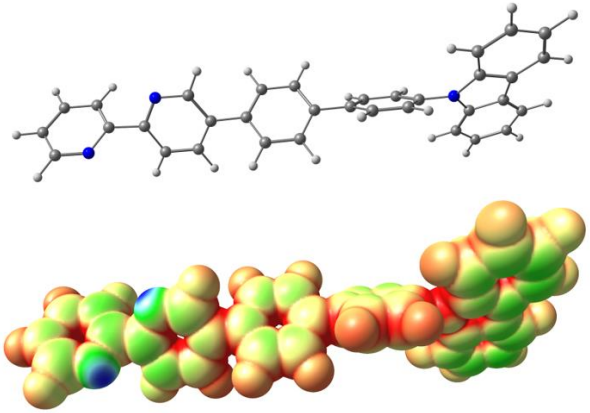

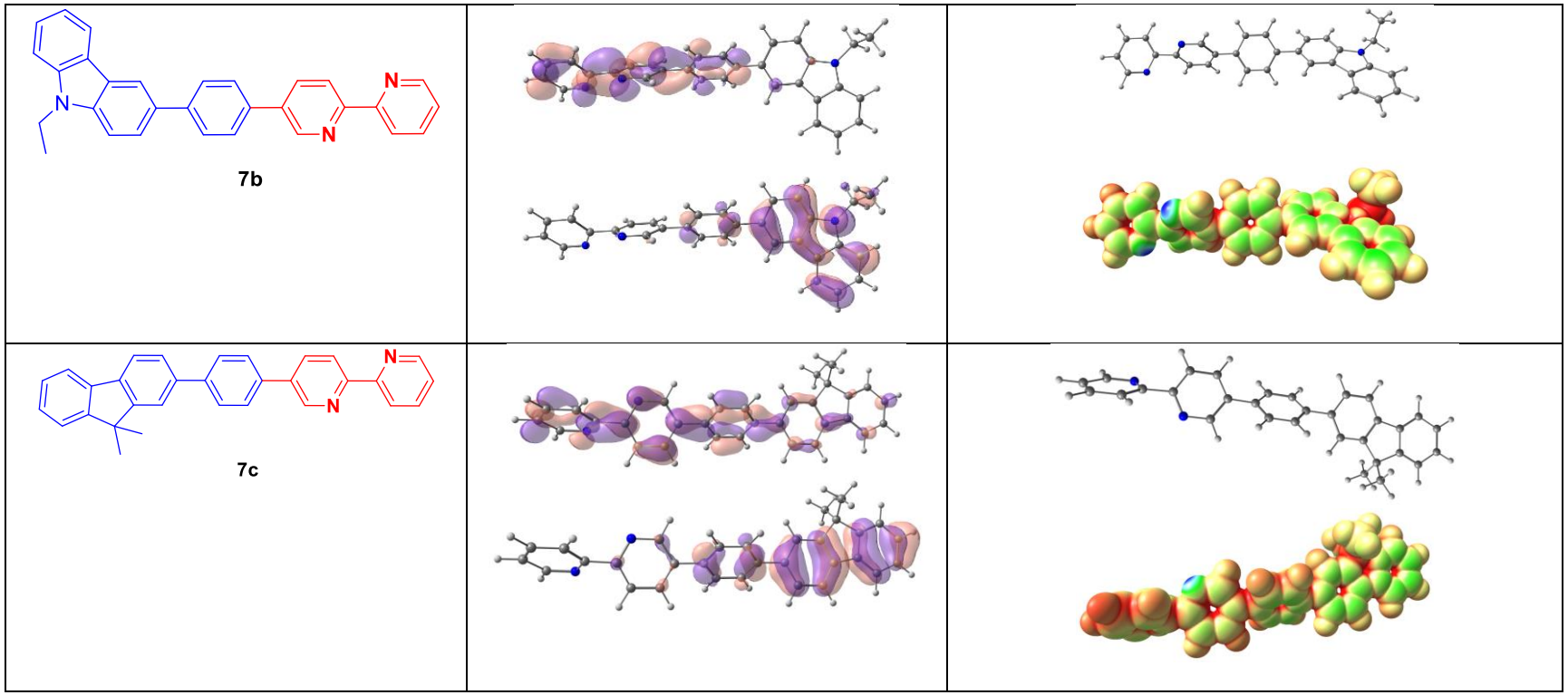

Table S9 The optimized geometries of **6a,b** and **7a,b** in MeCN

S	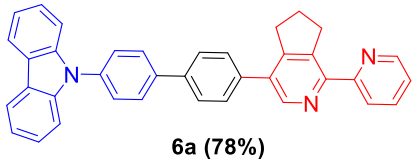 **6a (78%)**	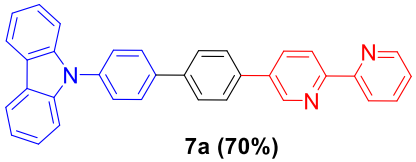 **7a (70%)**	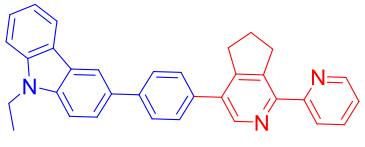 **6b (80%)**	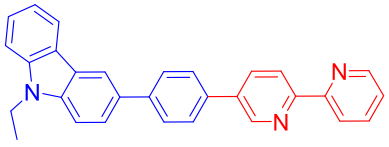 **7b (72%)**
S_0	119	125	119	120
S_1	94	119	121	120

Table S10 The optimized geometries of **6c** in cyclohexane/THF/MeCN

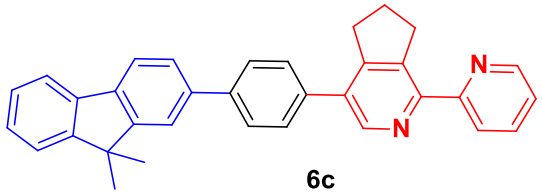

6c

S	Cyclohexane	THF	MeCN
S_0	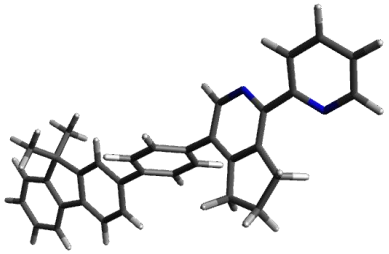	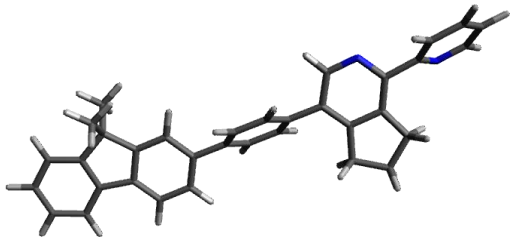	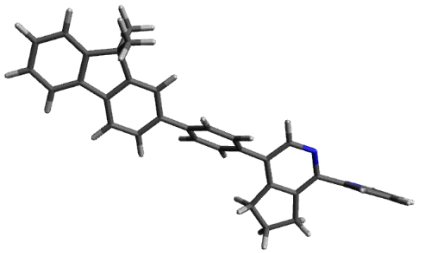
S_1	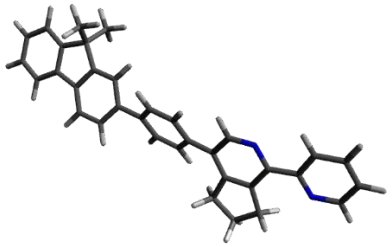	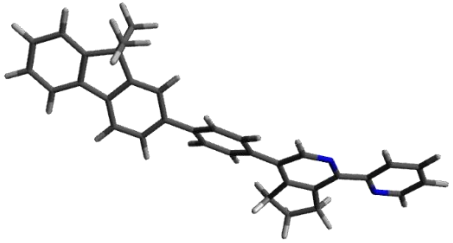	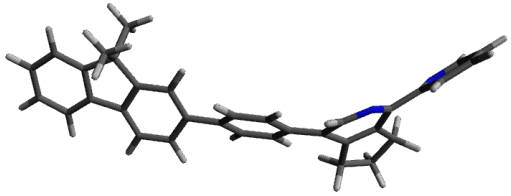

Table S11 The optimized geometries of 7**c** in cyclohexane/THF/MeCN

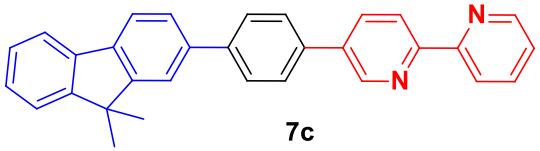

7c

S	Cyclohexane	THF	MeCN
S_0	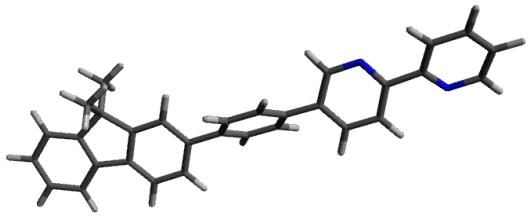	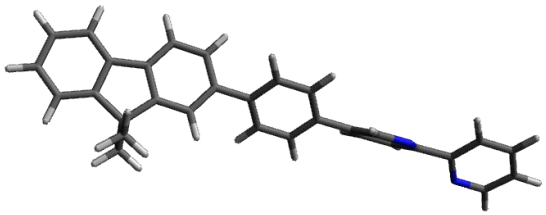	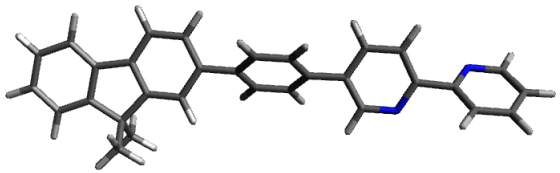
S_1	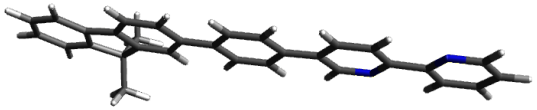	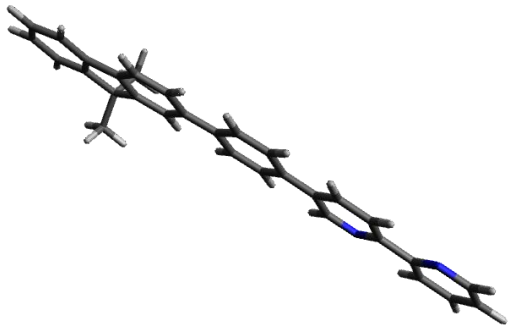	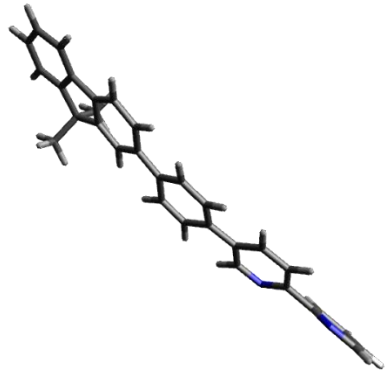

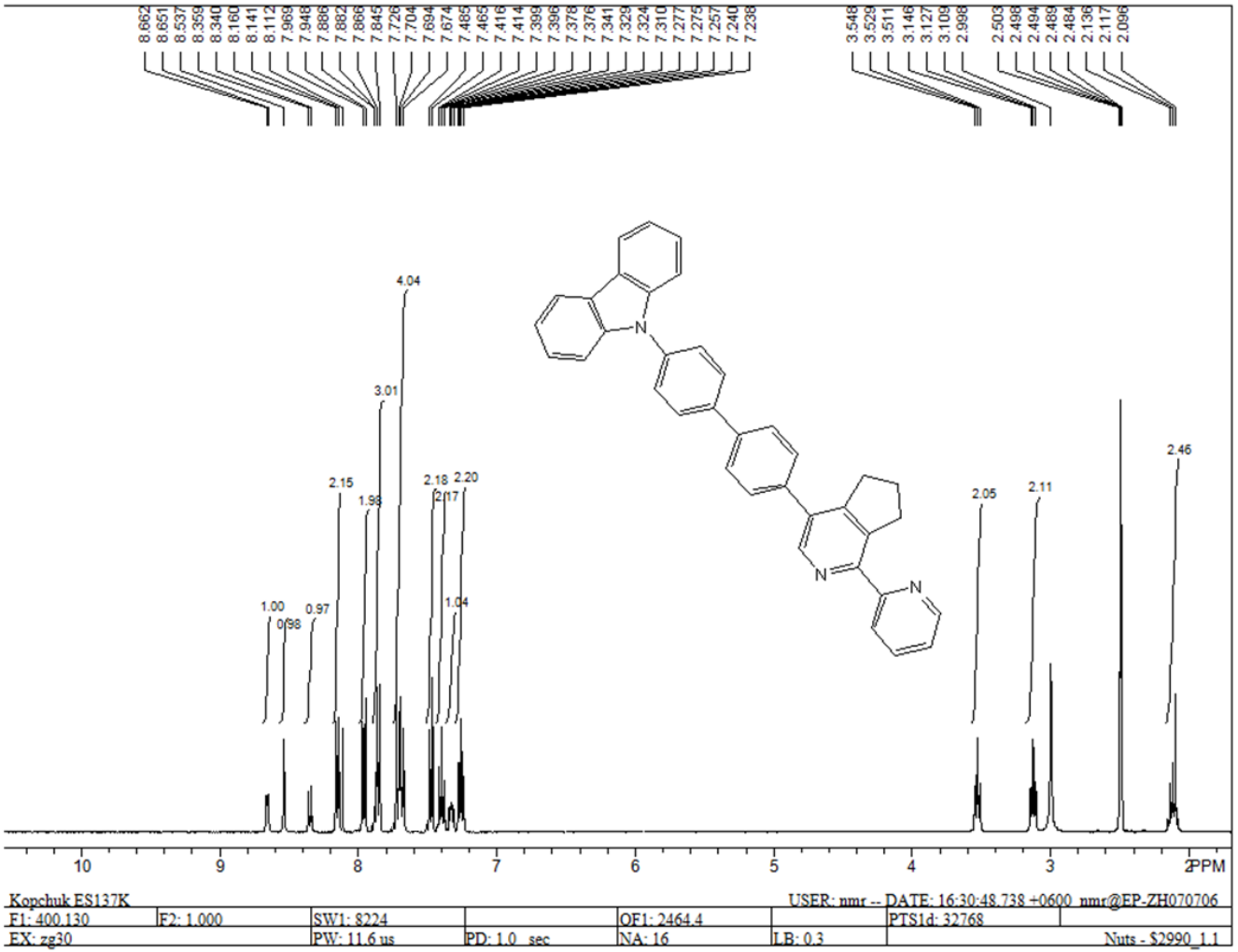

Figure S16 ^{1}H NMR of **6a** in DMSO -d6

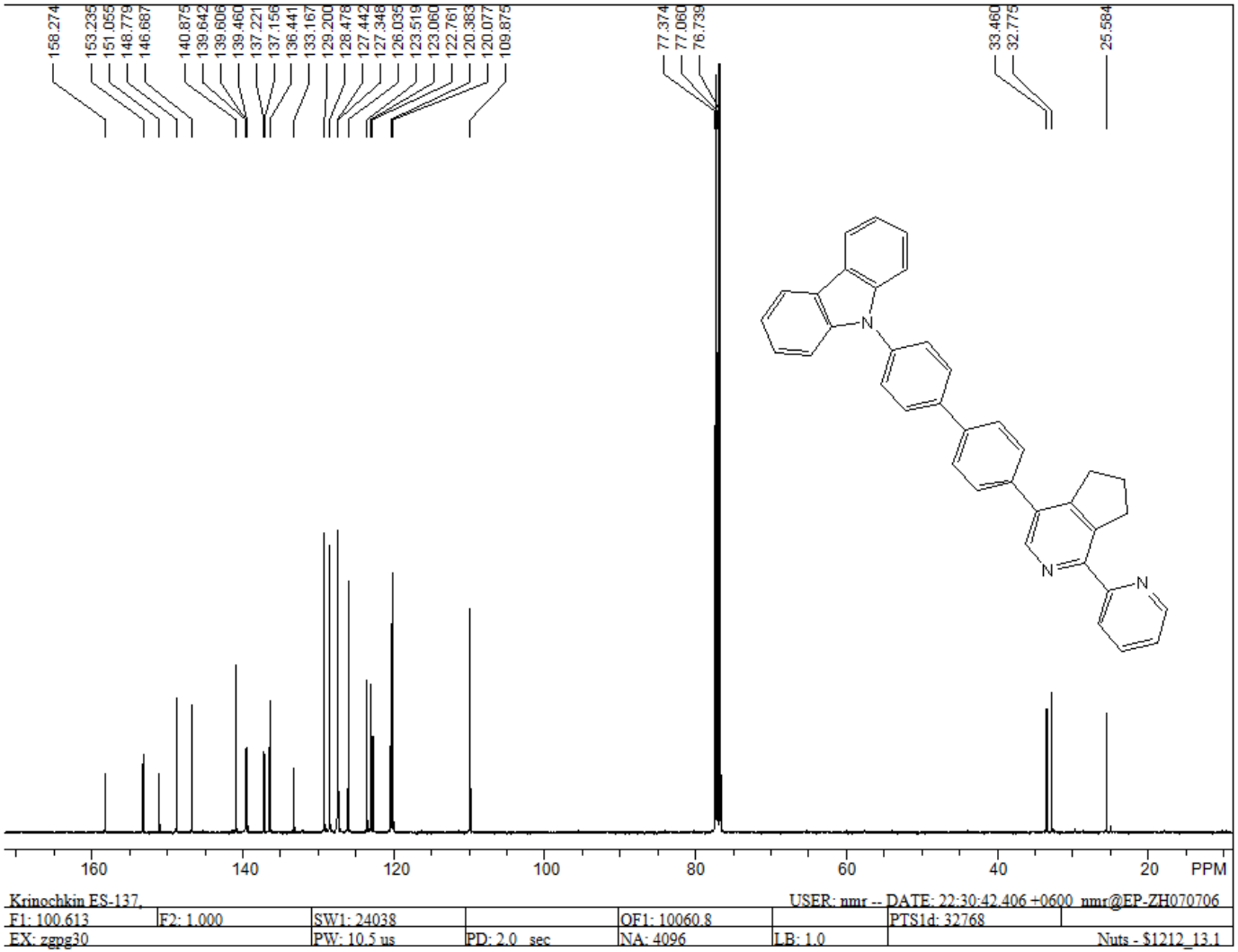

Figure S17. ^{13}C NMR of **6a** в $CDCl_3$

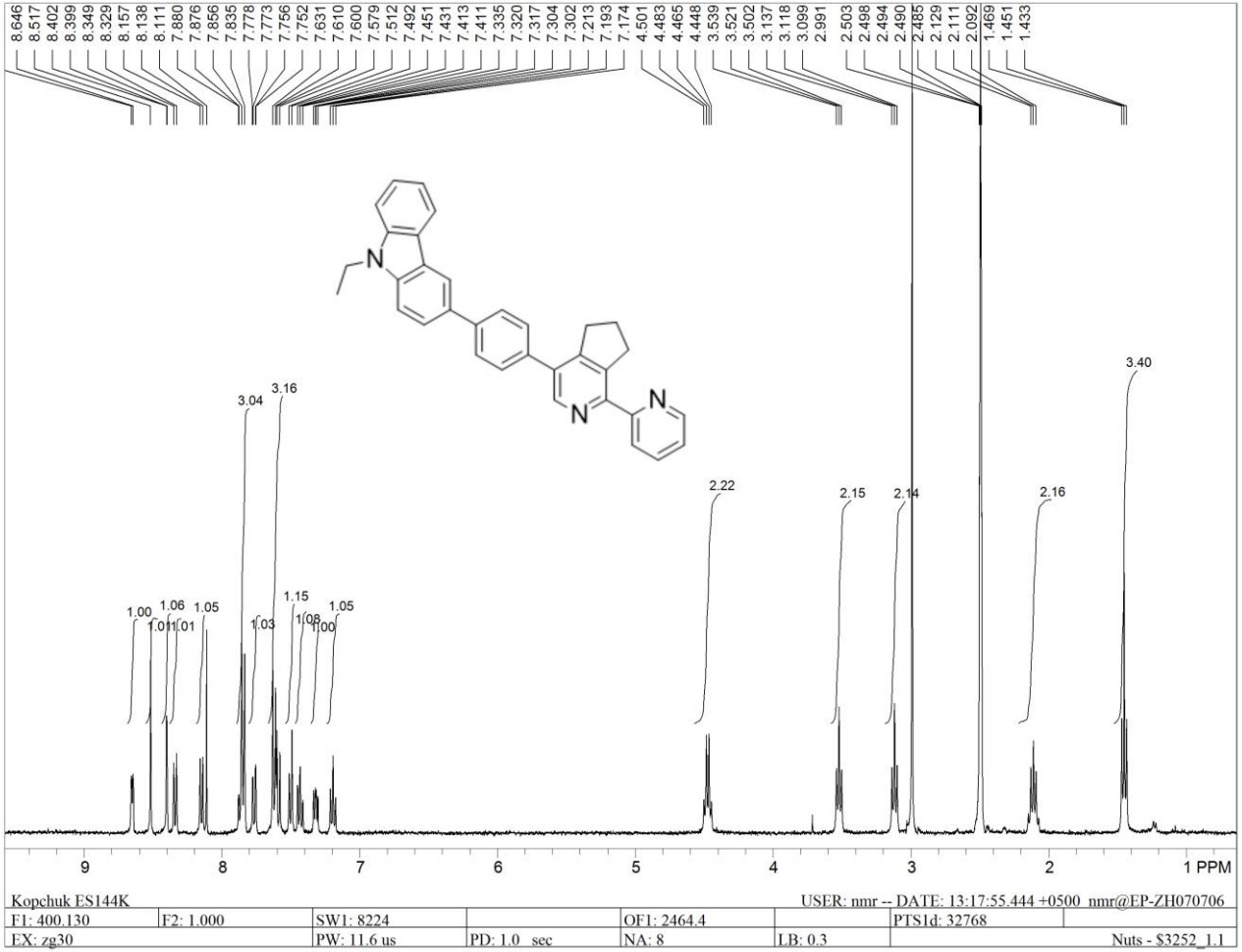

Figure S18. ^{1}H NMR of **6b** in DMSO-d_6

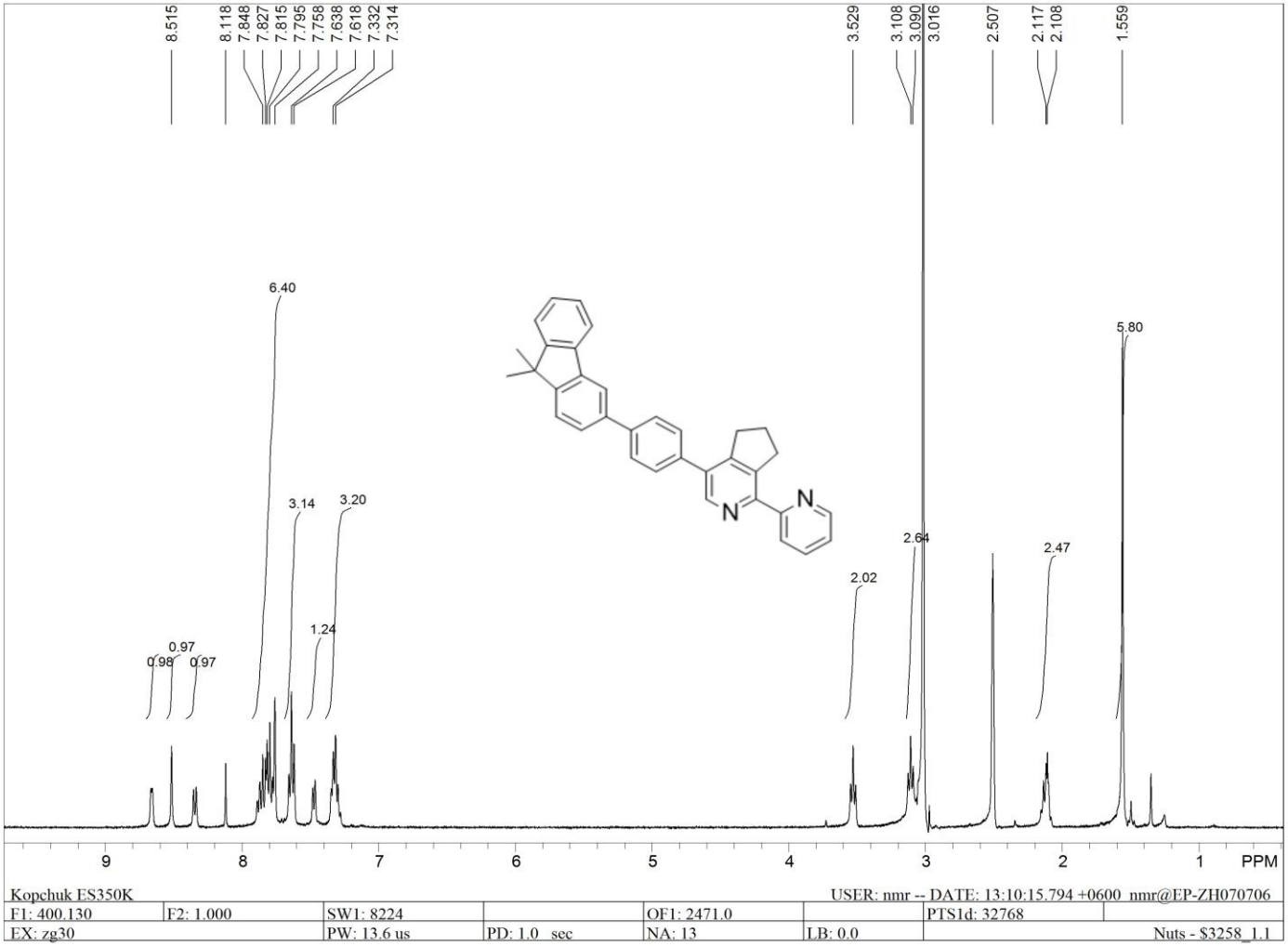

Figure S19. ^{1}H NMR of **6c** in DMSO-d_6

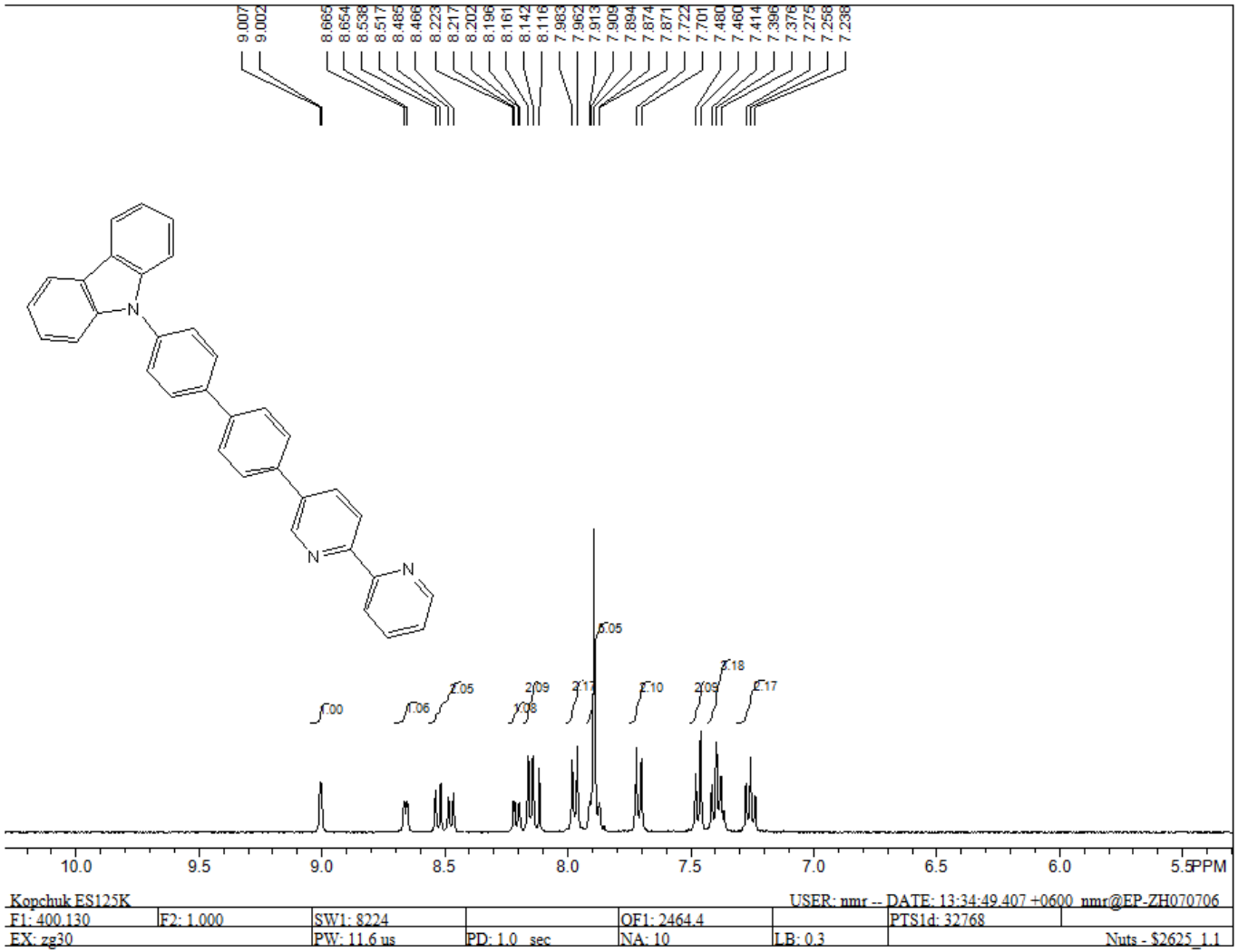

Figure S20 ^{1}H NMR of **7a** in DMSO -d6

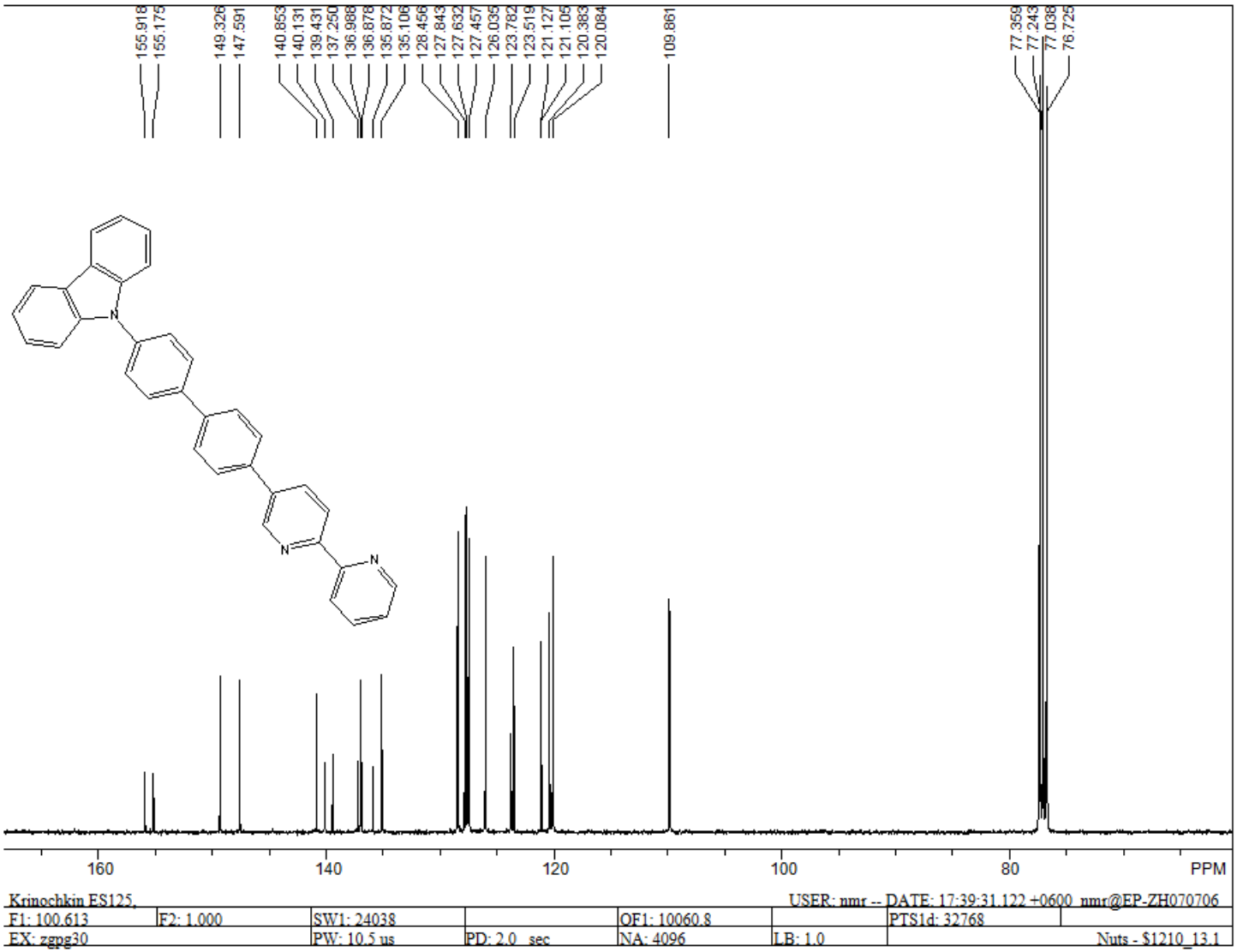

Figure S21 ^{13}C NMR of **7a** in $CDCl_3$

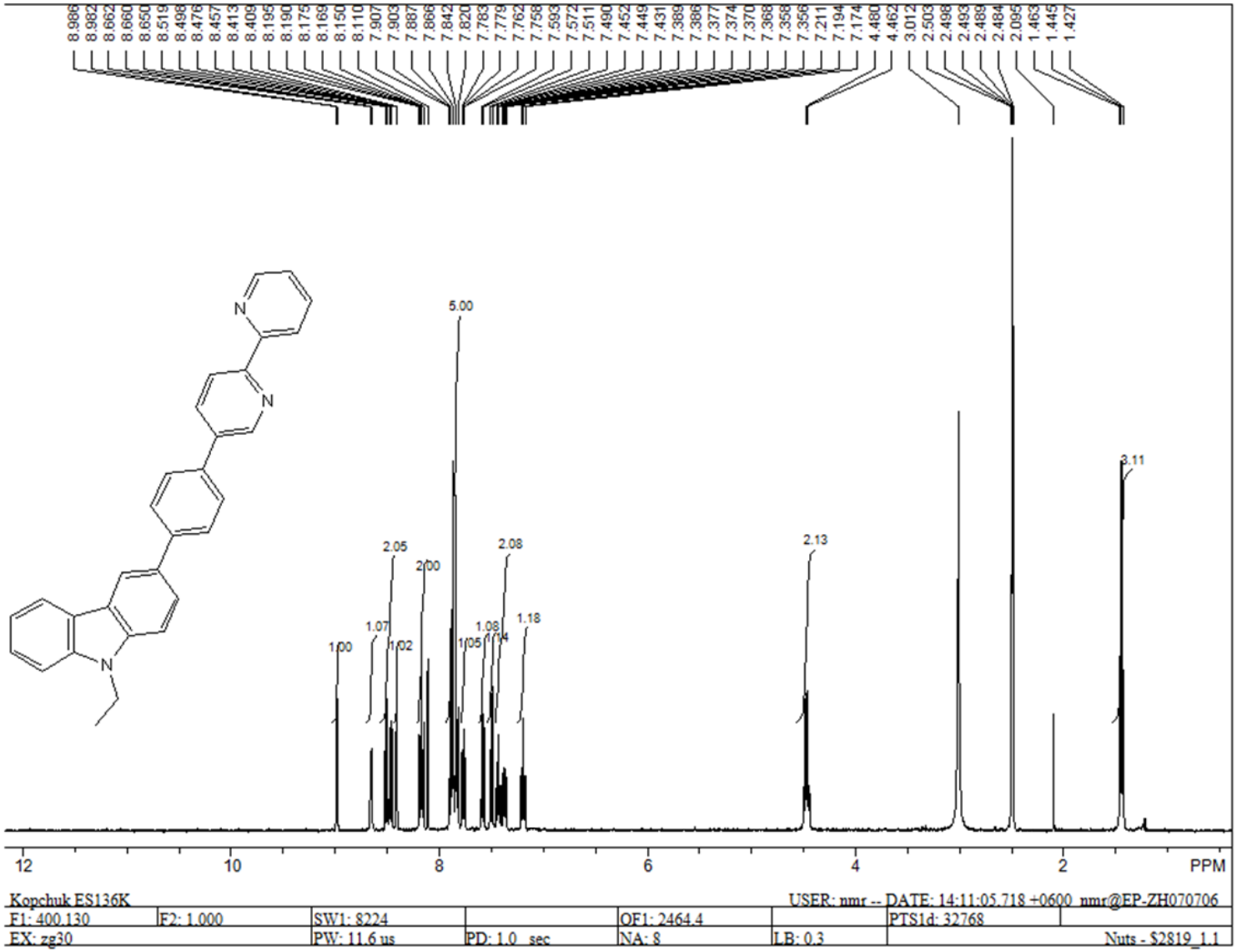

Figure S22 ^{1}H NMR of **7b** in DMSO -d6

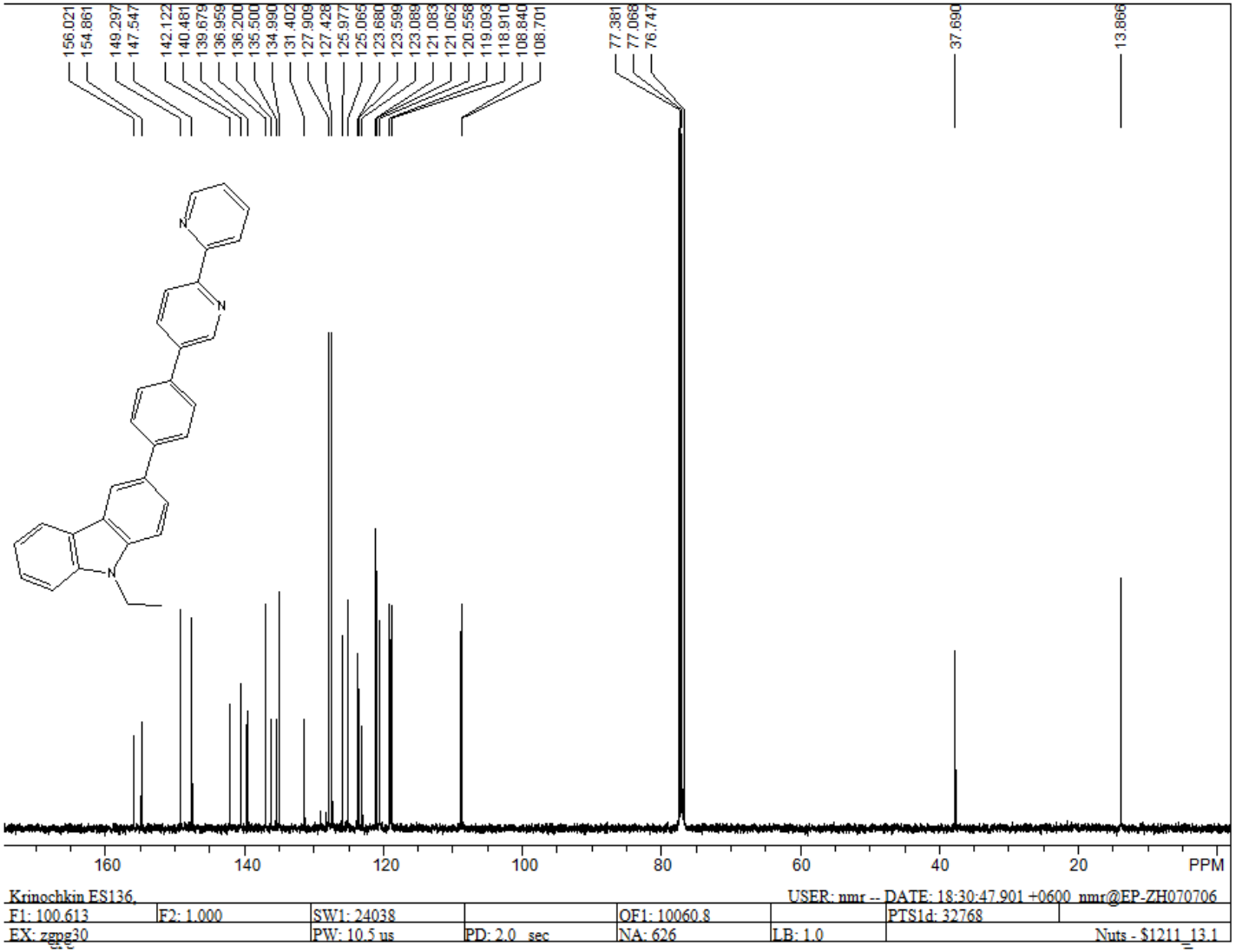

Figure S23 ^{13}C NMR of **7b** in $CDCl_3$

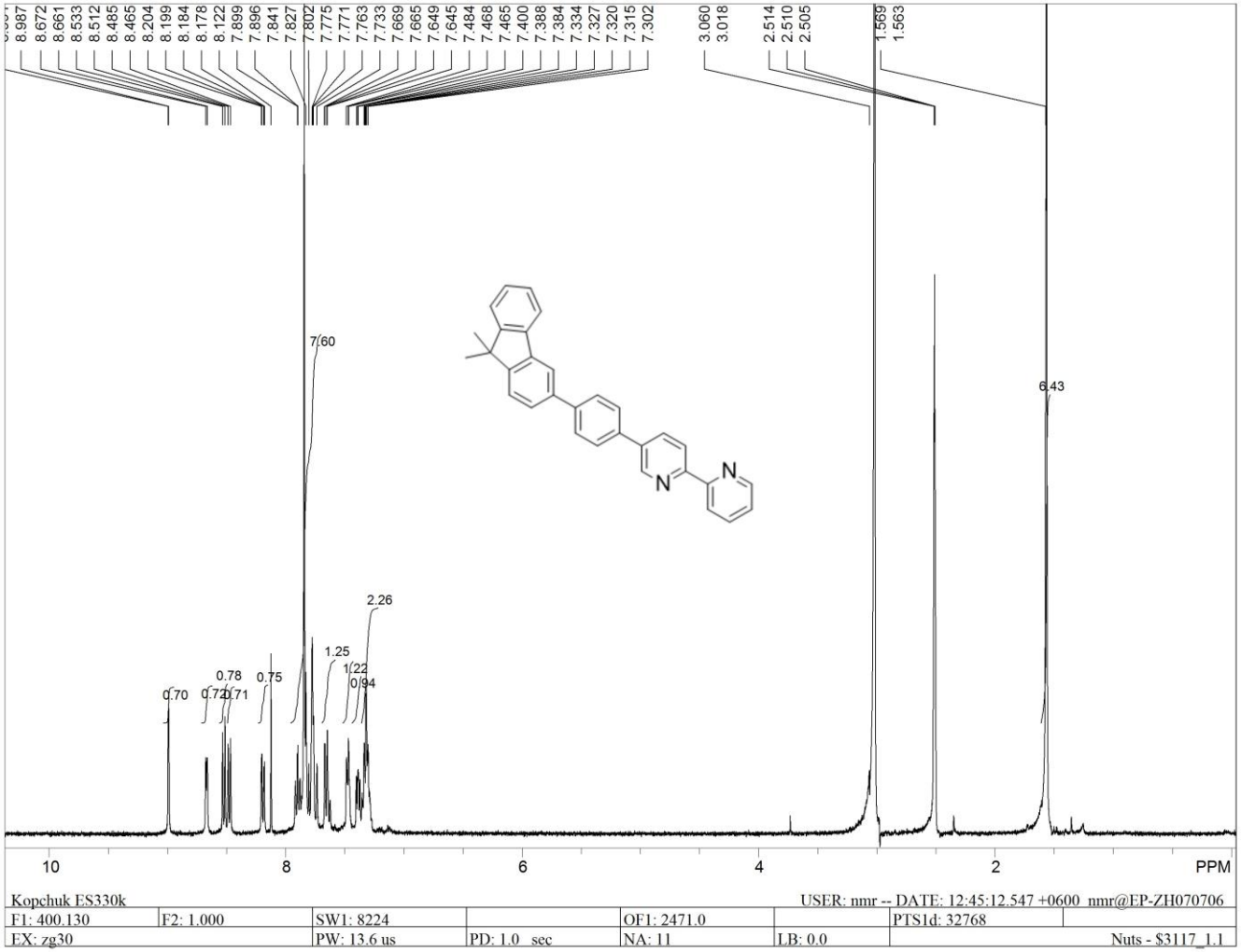

Figure S24. ^{1}H NMR of **7c** in DMSO-d_6

References

1 E. S. Starnovskaya, D. S. Kopchuk, A. F. Khasanov, O. S. Tanya, S. Santra, K. Giri, M. Rahman, I. S. Kovalev, G. v Zyryanov, A. Majee and V. N. Charushin, *Dyes and Pigments*, 2019, **162**, 324–330.

2 O. V. Shabunina, D. Yu. Kapustina, A. P. Krinochkin, G. A. Kim, D. S. Kopchuk, G. v. Zyryanov, F. Li and O. N. Chupakhin, *Mendeleev Communications*, 2017, **27**, 602–604.